Journal of Materials and Environmental Science
ISSN : 2028-2508
e-ISSN : 2737-890X
CODEN : JMESCN

J. Mater. Environ. Sci., 2024, Volume 15, Issue 11, Page 1516-1525

http://www.jmaterenvironsci.com

Studies of Electronic and Vibrational Properties of Nickel Sulphide Using First Principle Calculation Method

Clement H. N. [1]*, Tonga S. T. [2*], Idu H. K. [3], Danladi A .[4,] Sweta G. [5], Galadima T. [6]

[1*,2*,3,4] *Department of Physics, Taraba State University, Jalingo, P. M. B. 1167, Jalingo, Nigeria*
[5]*Department of Applied Physics, Gautam Buddha University, GautamBudhha Nagar, U. P. 201312, India.*
[6]*Department of Pharmaceutical Technology, Taraba State Polytechnic Suntai, Jalingo Campus, Taraba State, Nigeria.*

*[1]*Corresponding author, Email address: clementhyelnasinyi@gmail.com*
*[2]*Corresponding author, Email address: tahiru.tonga@tsuniversity.edu.ng*

Received *02 Oct 2024,*
Revised *29 Oct 2024,*
Accepted *01 Nov 2024*

Citation*: Clement H. N., Tonga S. T., Idu H. K., Danladi A., Sweta G., and Galadima T. (2024) Studies of Electronic and Vibrational Properties of Nickel Sulphide Using First Principle Calculation Method, J. Mater. Environ. Sci., 15(11), 1516-1525*

Abstract: Understanding the electronic and vibrational characteristics of materials is crucial for tailoring their properties for various applications. This study, employed Density Functional Perturbation Theory (DFPT) to investigate the electronic and vibrational modes of Nickel Sulphide (NiS) in its pristine state and under photo-doping conditions, where fractions of electrons are excited from the valence to the conduction band. Results revealed intriguing insights into the interplay between electronic excitations and phonon vibrations in NiS. Despite the photo-doping-induced changes in phonon vibrations, NiS retains its metallic nature, as evidenced by the consistent electronic properties observed in the density of states (DOS) and band structure (BS) analyses. Notably, the electronic band crossing the Fermi line confirms the metallic character. However, our findings suggest that NiS may not be suitable for semiconductor applications due to its unchanged electronic properties post-doping. This comprehensive study sheds light on the fundamental behaviour of NiS and provides valuable insights for potential applications in electronic devices.

Keywords: *Band structure; Density of states; Electronic structure; Phonon; Density Functional Theory; photo-doping*

1. Introduction

Nickel is an essential component for numerous applications in contemporary infrastructure and technology (Mudd, 2010). It is widely utilized in the aerospace industry, alloy production, and electroplating, among other fields, due to its outstanding physical and chemical characteristics (Kuck, 2012). In recent years, energy storage and conversion technologies have gained significant attention (Shao *et al.* 2022). Several technologies, including lithium–air batteries (LABs), lithium–sulfide batteries (LSBs), lithium-ion batteries (LIBs), sodium ion batteries (SIBs), potassium-ion batteries

(PIBs), zinc-ion batteries, zinc–air batteries, and supercapacitors (SCs), have been developed (Pothu *et al.* 2020). Supercapacitors, renowned for their high power density, excellent cycle stability, and environmental friendliness, are particularly valued in emerging energy technologies (Pothu *et al.* 2021).

Nickel sulfides have received extensive interest for super capacitor applications due to their specific advantages (Li *et al.* 2019). However, their electrochemical performance is significantly constrained by the distribution of electrochemically active sites. According to (Ripley *et al.* (2015), various strategies, such as constructing synergistic structures with conductive substrates, enhancing active sites through nanocrystallization, and creating nanohybrid architectures with other electrode materials, have been implemented to overcome this limitation (Pothu *et al.* 2020). Additionally, nickel sulfides are crucial in the formation of magmatic Ni-Cu-PGE sulfide deposits, aiding material circulation.

The synthesis of nickel sulphide thin films has been explored using various techniques, such as successive ionic layer adsorption and reaction (SILAR) and chemical bath deposition (Singh *et al.* 2018). These methods have demonstrated the ability to produce high-quality, nanostructured nickel sulphide materials with tailored properties (Asif *et al.* 2020). The transition metal sulphides, including nickel sulphide, have emerged as attractive semiconducting materials due to their direct band gaps, high absorption coefficients, and unique structural morphologies (Sleman, 2018; Tigwere *et al.* 2023; Alhassan *et al.* 2024).

A considerable share of the global nickel reserves, specifically 40%, is contained within magmatic sulfide deposits, where nickel sulfides are prevalent (Kuck, 2006). Key nickel sulfide minerals such as Millerite (NiS), heazlewoodite ($Ni3S_2$), and polydymite ($Ni3S_4$) are thermodynamically stable and extensively found in mantle peridotite (Zhang *et al.* 2020). Nickel sulfides have attracted interest because of their fundamental properties, industrial applications, and their role in material cycling (Zhang *et al.* 2020). Industrial uses include semiconductors, rechargeable lithium batteries, solar cells, and supercapacitors (Zang *et al.* 2020).

Experimental research by (Wang *et al.* 2007) has shown that four nickel sulfides are more stable than other forms. These include heazlewoodite Ni_3S_2, millerite NiS, polydymite Ni_3S_4, and pyrite NiS_2, ranging from nickel-rich to sulfur-rich compositions. The crystal structures of these sulfides have been thoroughly investigated: Ni_3S_2 has a stable rhombohedral structure, NiS has a hexagonal structure, and Ni_3S_4 and NiS_2 have cubic structures. However, the vibrational spectra of Ni-rich sulfides have not been completely characterized.

Ni_3S_2, synthesized through the impregnated thiosalt decomposition method, showed no Raman active lines when excited at 514.5 nm from an Ar-ion laser. In contrast, standard Ni_3S_2 from Aldrich displayed ten Raman peaks in the range of 140–438 cm^{-1}. For NiS, different Raman peak observations have been reported, with (Shen *et al.* 2003) detecting five peaks below 400 cm^{-1} in synthesized NiS nanorods, while (Bishop *et al.* 2000) identified eight peaks in highly purified NiS powder from Johnson Matthey GmbH.

The Raman spectra of sulfur-rich compounds $Ni3S_4$ and NiS_2 have been more consistently documented in previous studies. However, a thorough characterization of the vibrational properties of these compounds is necessary for accurate interpretation of Raman spectra. This is especially important for identifying nickel sulfides on Ni-based anode surfaces under solid oxide fuel cell (SOFC) operating conditions using in-situ Raman spectroscopy, as emphasized by (Cheng & Liu, 2007).

2. *Model and Computational Details*

The current computations were executed utilizing the Quantum Espresso Package (Giannozzi *et al.* 2017), employing the projector augmented-wave (PAW) method (Blöchl, 1994; Kresse & Joubert, 1999). The exchange-correlation functional was determined using the generalized gradient approximations (GGA) within the Perdew-Burke-Ernzerhof (PBE) framework (Perdew *et al.* 1996). Following a meticulous convergence analysis, we determined that an energy cutoff of 60 eV and a k-point mesh of $6 \times 6 \times 18$, generated via the Monkhorst–Pack scheme (Monkhorst & Pack, 1974), ensured convergence accuracy with total energy variations of less than 1 $meV/atom$. The crystal cell and internal parameters were optimized using the conjugate gradient method until the total force on each ion was below 0.05 $eV/$Å. The density of states (DOS) calculations were conducted using the tetrahedron method with Blöchl corrections (Blöchl, 2003), and the Fermi surfaces were visualized using Xcrysden (Kokalj A, 2003). Millerite NiS crystallizes in the R3m space group, forming a rhombohedral lattice with three NiS formula units used in the calculations. The computed lattice parameters for the crystal structure are $a = b = 9.50$ Å, indicating a hexagonal crystal structure, with a $\frac{c}{a}$ ratio of 3.13. These values are close to the theoretical data ($a = 9.60831$ Å, $c = 3.14445$ Å) provided by (Zhang *et al.* 2014) and align with experimental data ($a = 9.607$ Å, $c = 3.143$ Å) from (Rajamani & Prewitt, 1974), which were subsequently used in further calculations. The phonon calculations were carried out using a supercell method with finite displacements, as implemented in the Phonopy code (Togo *et al*. 2010). A $4 \times 4 \times 4$ supercell with 9 atoms and a displacement setting of 0.01 Å from the equilibrium atomic position was employed.

3. Results and Discussion

3.1 *Electronic Band Structure and Fermi surface of Nickel Sulphide.*

The electronic band structure of nickel sulphide refers to the arrangement of energy bands formed by the electrons in the material. According to (Zhang *et al.* 2014), the electronic structure of millerite NiS has been investigated using electron spectroscopic measurements and band structure calculations, which indicate millerite is highly covalent metal. Figure 1 shows the calculated band structure of NiS, the result obtained shows that, the bands from the valence band crosses the Fermi level indicate that, some electrons can move from the valence band to the conduction band which now signify the material ability to conduct electricity.

3.2 *Density of State of Nickel Sulphide*

This study investigated the electronic properties of Nickel Sulphide (NiS) both in its free state and when subjected to electron excitation. In its free state as shown in Figure 2a NiS was found to exhibit metallic properties as it shows the highest peak occur at the standard Fermi energy value of $\mathbf{12.43\ eV}$, as indicated by the DOS and the absence of a distinct bandgap in the electronic structure. The DOS plot revealed a continuous distribution of electronic states across the energy spectrum, consistent with the behavior of metallic materials. This suggests that, NiS allows for the free movement of electrons, contributing to its metallic conductivity. Upon electron excitation or photo-doping, the electronic properties of NiS were further investigated. Interestingly, despite the introduction of additional electrons through excitation, the material still retained its metallic behavior as shown in Figure 2b, it still shows the highest peak occur at the standard Fermi energy level of $\mathbf{12.43\ eV}$.

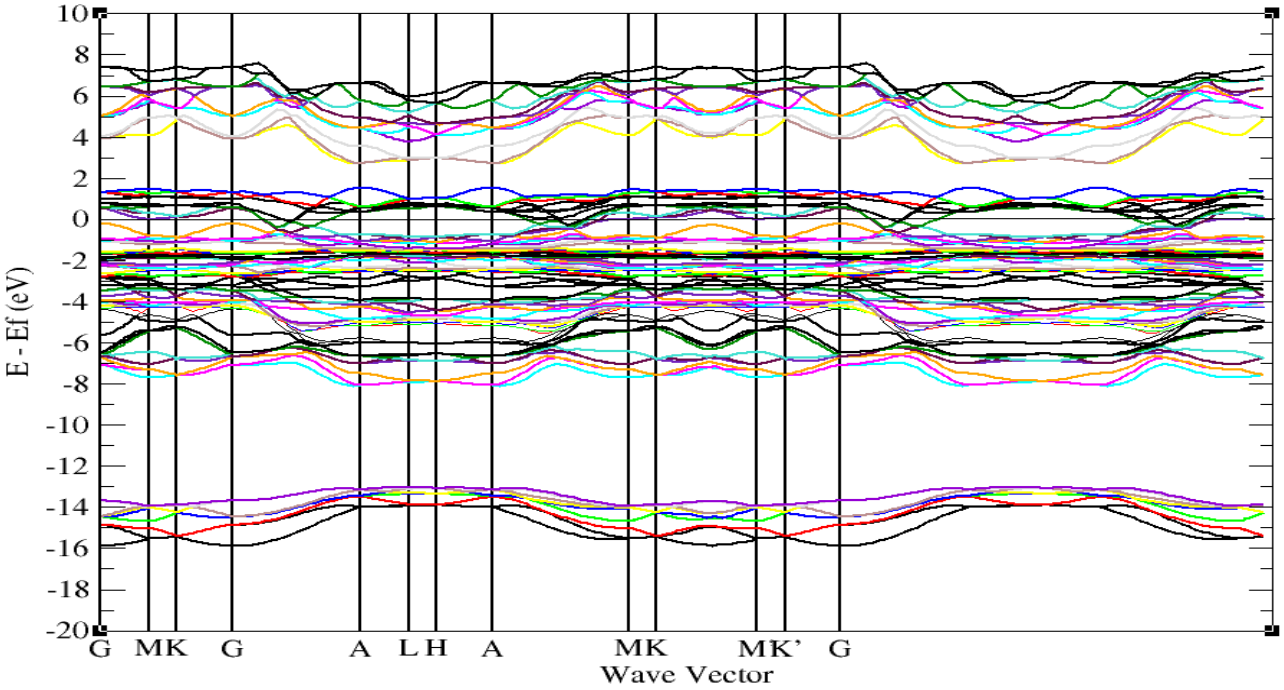

Figure 1. *Electronic Band Structure of Nickel Sulphide (ω vs k)*

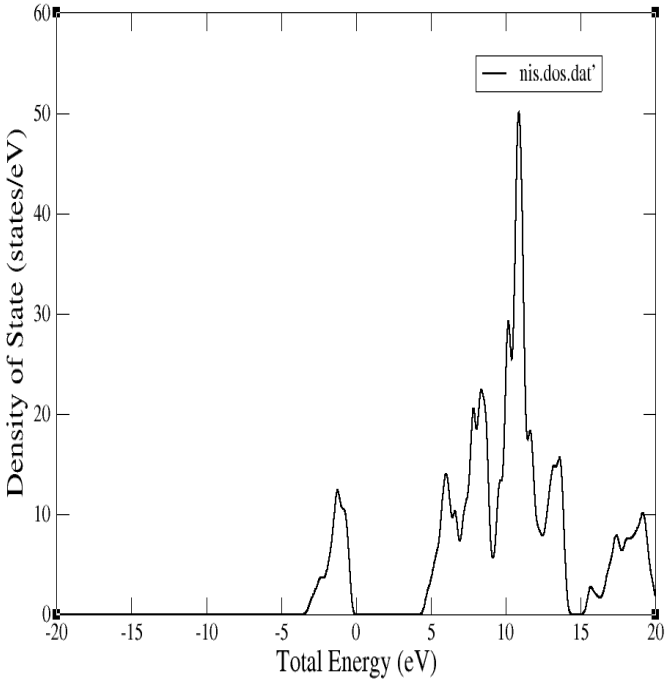

Figure 2a. Phonon Structure of photo-undoped

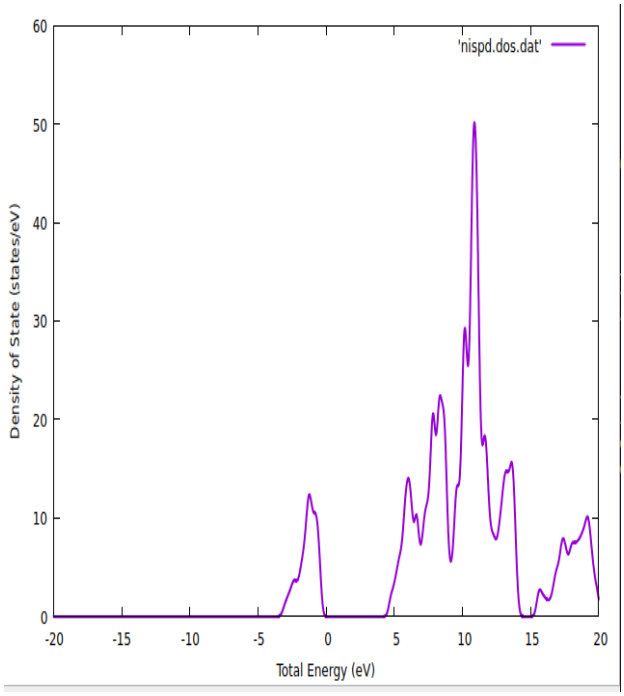

Figure 2b. Phonon Structure of photo-doped

3.3 *Projected Density of State*

Firstly, we give the detailed electronic structure. The orbital projected density of states (PDOS) are shown in Figure 3. The PDOS below about $-3.8\ eV$ is mainly contributed by S-2p. Ni-3d and S-3p states are found to be hybridized strongly in the range from $-8.0\ eV\ to\ -3.5\ eV$. The DOS from $-3.5\ eV$ to about $-1.0\ eV$ is dominated by the Ni-3d contribution, while the region from $-1.0\ eV$ to about $1.4\ eV$ near the Fermi level is mainly hybridized with Ni 3d and S-3p. It is apparent that the electronic states near Fermi level mainly consist of Ni-3d and S-3p orbital, which confirms the

millerite NiS is a highly covalent pd metal. The results are in line with earlier experimental and theoretical study (Zhang *et al.* 2014), which also suggests that the strong hybridization between Ni-3d and S-2p orbitals leads to metallic behavior of millerite NiS.

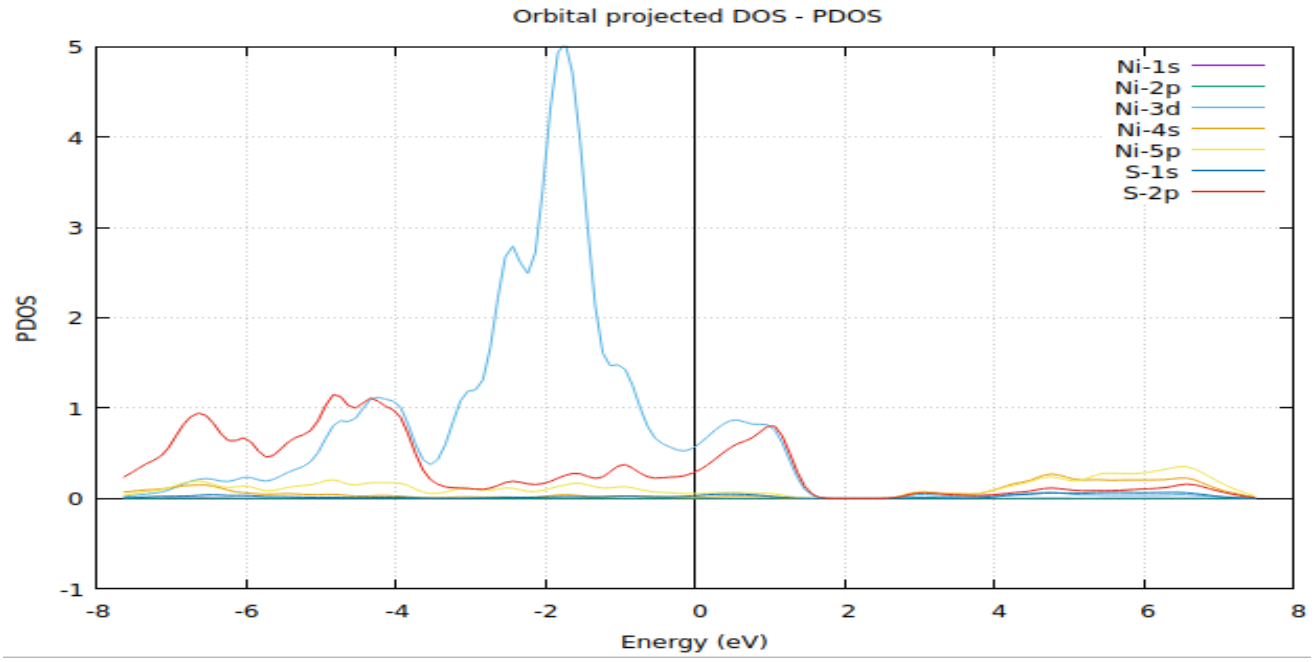

Figure 3. Orbital Projected Density of State of Nickel Sulphide.

3.4 *Phonon Bands Structure at Γ Point.*

The ground-state electronic structure of Nickel Sulfide (NiS) was analyzed by computing its electronic band structure at the Γ point. The band structure provides a detailed depiction of energy levels and electronic transitions within the crystal lattice. Figure 4 shows distinct electronic bands with varying energy levels, indicating NiS's electronic behavior in its equilibrium state.

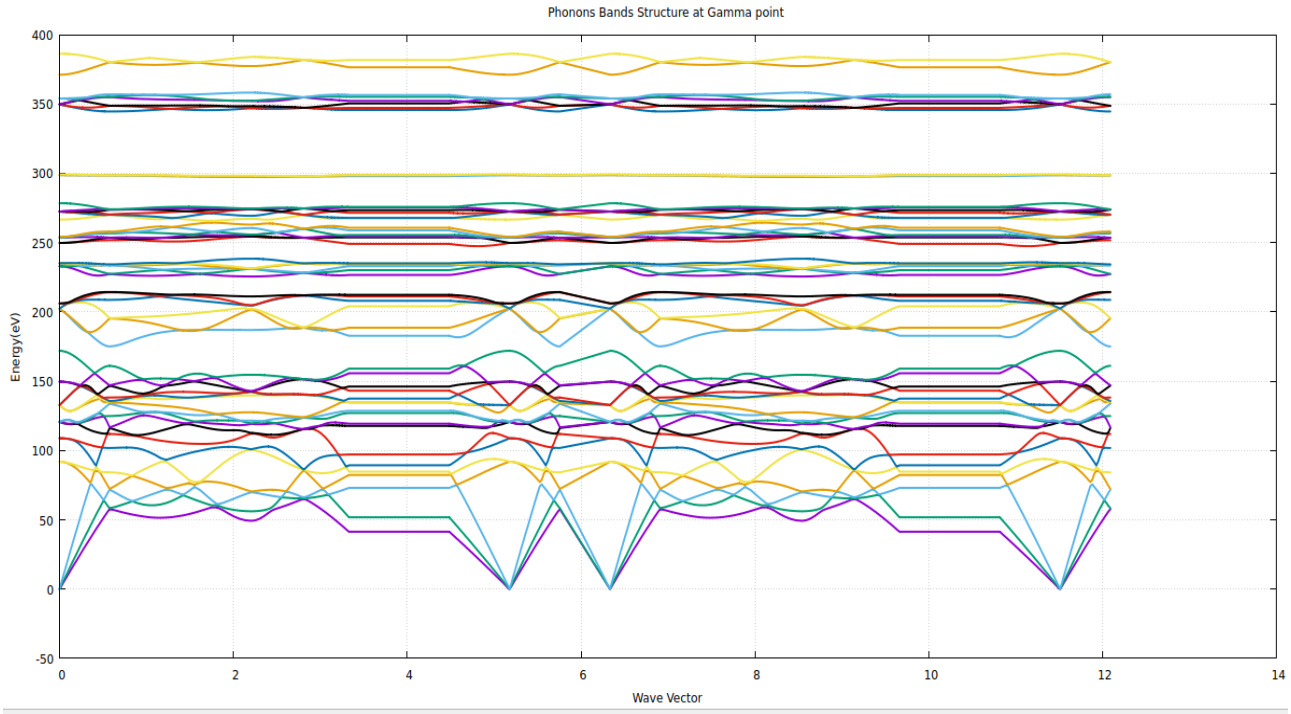

Figure 4. Phonon Bands Structure at **Γ** Point

The band structure, which describes the distribution of electron energy levels relative to their momentum, offers perceptivity into electron behavior and their interaction with photons. In semiconductors, the valence band (fully occupied by electrons at absolute zero) and the conduction band (where electrons can move freely) are fundamental. For the NiS, the phonon band structure at the Γ point reveals a zero band gap, indicating metallic properties since the valence and conduction bands overlap. In materials science, the presence or absence of a band gap is crucial. Semiconductors and insulators have a non-zero band gap that dictates their electrical conductivity, while a zero band gap, as in NiS, allows free electron movement, resulting in metallic conductivity. This continuous band of electronic states facilitates electron delocalization, enabling easy movement in response to an external electric field.

3.5 *Structural optimization*

In this study, we use Nickel Sulphide (NiS) in its primitive cell having 9 atoms of nickel and 9 atoms of sulphur in a hexagonal structure with braivais lattice index of 4. Figure 5. illustrate the crystal structure of Nickel Sulphide (NiS). The crystal structure was visualized using VESTA software as shown in Figure 5.

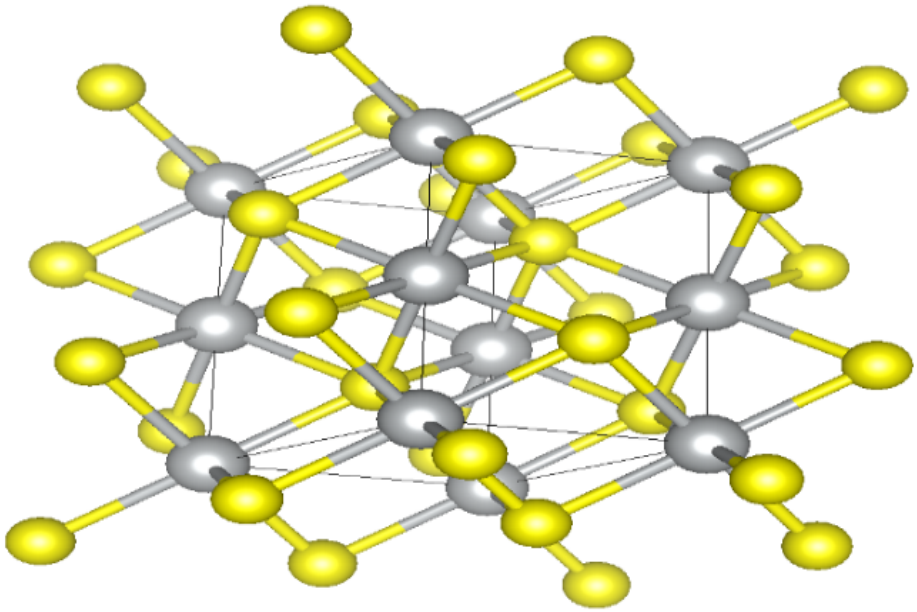

Figure 5. The crystal structure of Nickel Sulphide. The grey spheres represent Nickel (Ni) while the yellow spheres represent Sulphur (S).

3.6 *Phonon Calculations*

The force constants matrix was calculated by perturbing each atom in the crystal lattice and calculating the resulting forces and also the phonon dispersion by di**a**gonalizing the force constants matrix to obtain phonon frequencies and modes for the doped and undoped, which represent vibrational motions as shown in the Table 1 and Table 2 and these frequencies were varied at different modes and significant changes was observed in the phonon modes. Following the Phonon frequency mode of the doped and un-doped NiS, we further explore its phonon modes at first, second, third and forth frequencies of the unphoto-doped and the photo-doped to show the vibrational modes of the NiS after photo-doping.

Table 1. Phonon frequency (un-doped).

S/N	Frequency (THz)	Frequency (Cm^{-1})
1	-0.000000	-0.000007
2	-0.000000	-0.000007
3	-0.000000	-0.000003
4	0.000000	0.000004
5	0.000000	0.000007
6	0.000000	0.000008
7	2.754810	91.890565
8	3.256307	108.618711
9	3.313461	110.525174
10	3.594861	119.911655

Table 2. Phonon frequency (doped).

S/N	Frequency (THz)	Frequency (cm^{-1})
1	-12.077197	-402.851936
2	-11.656561	-388.821035
3	-11.404515	-380.413670
4	-11.349921	-378.592616
5	-11.304728	-377.085141
6	-10.926370	-364.464463
7	-10.301143	-343.609136
8	-10.287860	-343.166074
9	-10.118755	-337.525351
10	-10.117866	-337.495674

The following structures displayed in Figure 6a, and 6b show that, in its undoped state, NiS typically demonstrates phonon modes where atoms vibrate in opposite directions within the unit cell, characteristic of optical phonons.

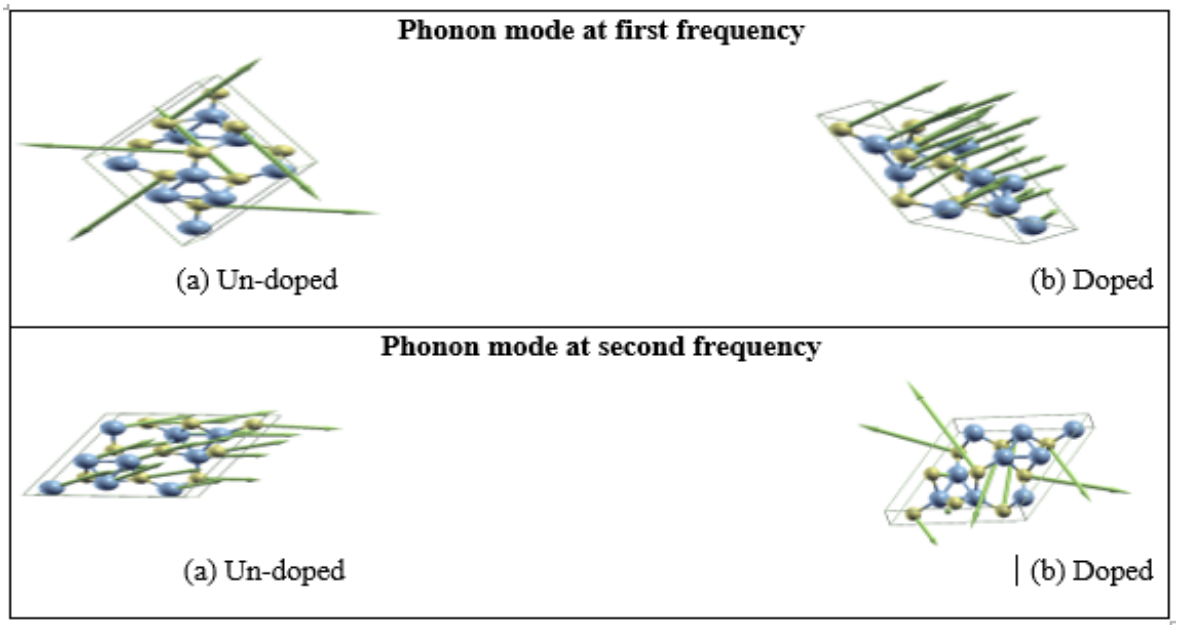

Figure. 6a Vibrational modes of NiS

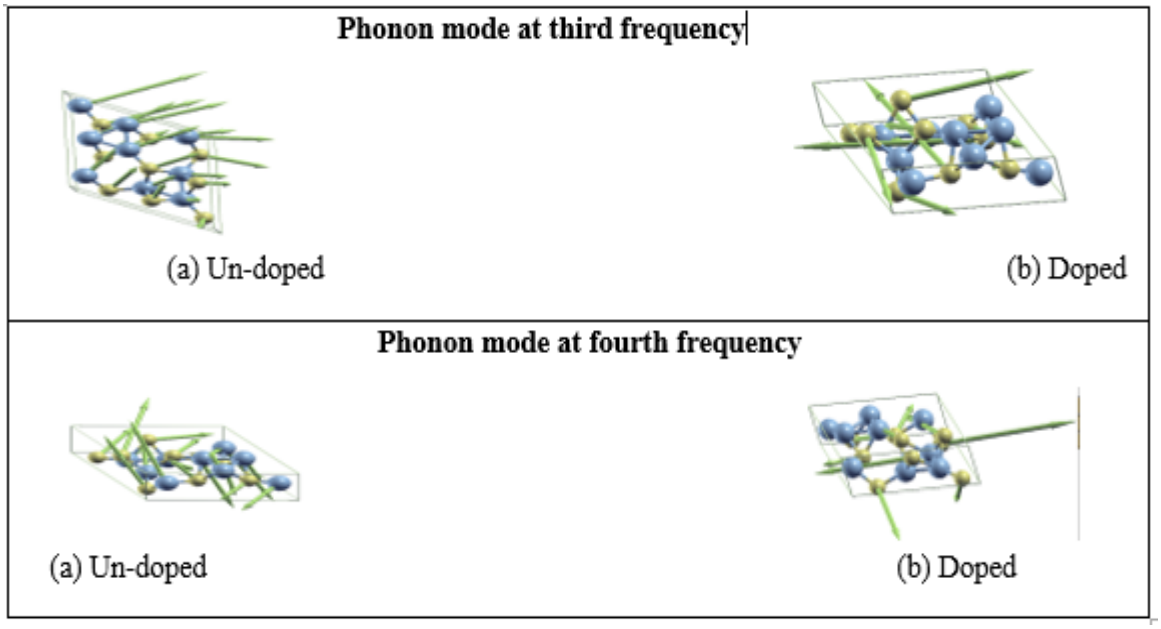

Figure. 6b Vibrational modes of NiS

The nickel (Ni) and sulfur (S) atoms oscillate against each other, resulting in high-frequency vibrational modes. This opposing movement is driven by the intrinsic force constants and bonding interactions within the crystal lattice. However, in some instances, undoped NiS may exhibit phonon modes where atoms vibrate in the same direction. This a typical behavior can arise from specific intrinsic properties of the material, such as unique electronic configurations or local bonding environments that promote synchronized atomic motion.

Conclusion

This study presents a comprehensive analysis of the electronic structure, Fermi surfaces, phonon dispersion, and transport properties of Nickel Sulphide (NiS) using first-principles calculations and Density Functional Perturbation Theory (DFPT). Results confirm that, millerite NiS is metallic, with structural parameters and density of states aligning well with experimental data. Despite photo-doping, NiS retains its metallic nature, as shown by consistent electronic properties in density of states (DOS) and Band Structure (BS) analyses. However, the unchanged electronic properties post-doping indicate that NiS is not suitable for semiconductor applications, underscoring the importance of understanding electronic behavior for material-specific applications.

This study enhances our understanding of NiS's fundamental properties and suggests potential applications in electronic devices. Future research should explore alternative materials or doping strategies for semiconductor applications, building upon the insights gained from this investigation.

Acknowledgement: The authors wish to acknowledge ICTP-East African Institute for Fundamental Research, University of Rwanda, Kigali for providing computational resources and the technical inputs of Dr. Mukthar Lawal of Max Planck Institute for the Structure and Dynamics of Matter, Hamburg, Germany.

Disclosure statement: *Conflict of Interest:* The authors declare that there are no conflicts of interest.
Compliance with Ethical Standards: This article does not contain any studies involving human or animal subjects.

References

Alhassan S., Alshammari A. H., Alotibi S., Alshammari K., Mohamed W. S., Hadia N. M. A. (2024) Structural and Optical Properties of Nickel-Doped Zinc Sulfide. *Nanomaterials,* 14(19), 1599. https://doi.org/10.3390/nano14191599

Asif, M., Ali, Z., Qiu, H., Rashad, M., & Hou, Y. (2020). Confined Polysulfide Shuttle by Nickel Disulfide Nanoparticles Encapsulated in Graphene Nanoshells Synthesized by Cooking Oil. *Figshare*.

Bishop, D. W., Thomas, P. S., & Ray, A. S. (1998). Raman spectra of nickel (II) sulfide. *MaterialsResearch Bulletin*, *33*(9), 1303-1306.

Bishop, D. W., Thomas, P. S., & Ray, A. S. (2000). Micro Raman characterization of nickel sulfide inclusions in toughened glass. *Materials Research Bulletin*, *35*(7), 1123-1128.

Blöchl, P. E., Jepsen, O., & Andersen, O. K. (1994). Improvedtetrahedronmethod for Brillouin-zone integrations. *Physical Review B*, *49*(23), 16223.

Cheng, Z., & Liu, M. (2007). Characterization of sulfur poisoning of Ni–YSZ anodes for solidoxide fuel cells using in situ Raman micro spectroscopy. *Solid State Ionics*, *178*(13-14), 925-935.

Giannozzi, P., Andreussi, O., Brumme, T., Bunau, O., Nardelli, M. B., Calandra, M., &Baroni, S. (2017). Advanced capabilities for materials modelling with Quantum ESPRESSO. *Journal of physics: Condensed matter*, *29*(46), 465901.

Kokalj, A. (2003). Computer graphics and graphical user interfaces as tools in simulations of matter at the atomic scale. *Computational Materials Science*, *28*(2), 155-168.

Kresse, G., & Joubert, D. (1999). From ultrasoft pseudopotentials to the projector augmented-wave method. *Physical review b*, *59*(3), 1758.

Kuck P. H. (2012) Mineral Commodity Summaries 2012: Nickel. *US Geological Survey.*

Kuck, P.H. (2006). Mineral Commodity Summaries; *U.S. Geological Survey:* Reston, VA, USA.

Li, X., Yan, W., Guo, S., Liu, Y., Niu, J., Yin, L., & Wang, Z. (2021). One-step electrochemical controllable preparation of nickel cobalt sulfide nanosheets and its application in supercapacitors. *Electrochimica Acta*, *387*, 138488.

Monkhorst, H. J., & Pack, J. D. (1976). Special points for Brillouin-zone integrations. *Physical review B*, *13*(12), 5188.

Mudd, G. M. (2010). Global trends and environmental issues in nickel mining: Sulfides versus laterites. *Ore Geology Reviews*, *38*(1-2), 9-26.

Perdew, J. P., Burke, K., & Ernzerhof, M. (1996). Generalized gradient approximation made simple. *Physical review letters*, *77*(18), 3865.

Pothu, R., Bolagam, R., Wang, Q. H., Ni, W., Cai, J. F., Peng, X. X., Ma, J. M. (2021). Nickel sulfide-based energy storage materials for high-performance electrochemical capacitors. *Rare Metals*, *40*, 353-373.

Pothu, R., Gaddam, S. K., Vadivel, S., & Boddula, R. (2020). Graphene-based materials for self-healable supercapacitors. *Mater. Res. Found*, *64*, 167-180.

Rajamani, V. T., & Prewitt, C. T. (1974). The crystal structure of millerite. *The Canadian Mineralogist*, *12*(4), 253-257.

Ripley, E. M., Dong, S., Li, C., & Wasylenki, L. E. (2015). Cu isotope variations between conduit and sheet-style Ni–Cu–PGE sulfide mineralization in the Midcontinent Rift System, North America. *Chemical Geology*, *414*, 59-68.

Shao, C., Zhao, Y., & Qu, L. (2022). Recent advances in highly integrated energy conversion and storage system. *Sus Mat*, *2*(2), 142-160.

Shen, G., Chen, D., Tang, K., An, C., Yang, Q., Qian, Y. (2003). Phase-controlled synthesis and characterization of nickel sulfides nanorods. *Journal of Solid State Chemistry*, *173*(1), 227-231.

Singh, N., Siwatch, P., Arora, A., Sharma, J., & Tripathi, S. K. (2018). SILAR deposition of nickel sulfide counter electrode for application in quantum dot sensitized solar cell. *AIP Conference Proceedings*.

Sleman, U. M. (2018). Synthesis and characterization of nanocrystalline copper sulfide powders. *Iraqi Journal of Physics*, *16*(38), 124–131.

Tigwere G. A., Khan M. D., Nyamen L. D., de Souza F. M., Lin W., Gupta R. K., Neerish Revaprasadu N., Ndifon P. T. (2023), Transition metal (Ni, Cu and Fe) doped MnS nanostructures: Effect of doping on supercapacitance and water splitting, *Materials Science in Semiconductor Processing,* 158, 107365, ISSN 1369-8001, https://doi.org/10.1016/j.mssp.2023.107365

Togo, A., Chaput, L., Tanaka, I., & Hug, G. (2010). First-principles phonon calculations of thermal expansion in $Ti_3 SiC_2$, $Ti_3 AlC_2$, and $Ti_3 GeC_2$. *Physical Review B*, *81*(17), 174301.

Togo, A., Oba, F., Tanaka, I. (2008). First-principles calculations of the ferro-elastic transition between rutile-type and CaCl 2-type SiO_2 at high pressures. *Physical Review B*, *78*(13), 134106.

Tonga, S. T., Baro, Y. J. (2022). Structural and Electronic Properties of Gallium Phosphate Semiconductor in Wurtzite Rock-Salt and Zinc-Blende. *International Journal of Engineering and Applied Physics*, *2*(3), 555-565.

Wang, J. H., Cheng, Z., Brédas, J. L., & Liu, M. (2007). Electronic and vibrational properties of nickel sulfides from first principles. *The Journal of Chemical Physics*, *127*(21).

Yang, Z. K., Wang, J. R., & Liu, G. Z. (2018). Effects of Dirac cone tilt in a two-dimensional Dirac semimetal. *Physical Review B*, *98*(19), 195123.

Zhang, Q., Tian, Y., Liu, S., Yang, P., & Li, Y. (2020). First-principles study of the elastic properties of nickel sulfide minerals under high pressure. *Minerals*, *10*(9), 737.

Zhang, W. B., Li, J., Liu, X. H., & Tang, B. Y. (2014). Electronic structure and thermodynamic properties of millerite NiS from first principles: Complex fermi surface and large thermal expansion coefficient. *Computational materials science*, *83*, 412-417.